Isoquinoline Containing Azo Schiff Derivatives as Potential Antitubercular Agents: Synthesis, Characterization, Molecular Docking, PASS Prediction and ADME Studies

S. Sahana[iD] and G.R. Vijayakumar[*,iD]

Department of Chemistry, University College of Science, Tumkur University, Tumakuru-572103, India

*Corresponding author: E-mail: vijaykumargr18@gmail.com

A series of isoquinoline containing novel azo Schiff base derivatives (**3a-l**) were synthesized and characterized by FT-IR, NMR (^{1}H NMR & ^{13}C NMR) and mass spectral analysis. The synthesized title compounds were evaluated for *in vitro* antitubercular activity against *Mycobacterium tuberculosis* (MTB) H37Rv strain by microplate alamar blue assay (MABA) method. Among the synthesized series of compounds, the compounds **3a**, **3b**, **3c** and **3d** were emerged as excellent antitubercular agents. Compound **3b** showed the lowest MIC value of 1.6 μg/mL with a potency equivalent to the standards, isoniazid and ethambutol. Compounds **3a** & **3c** showed MIC value of 3.125 μg/mL, which is equivalent to the activity of a reference standard pyrazinamide. Compound **3d** showed significant activity with MIC of 6.25 μg/mL and other compounds showed good to moderate activity ranging from 12.5 to 50 μg/mL. The four potent components were further tested for *in vitro* cytotoxicity using MTT assay against MCF-7 and HeLa cell lines to check the selectivity index. Among the tested series, compound **3b** possessed the highest cytotoxicity against both MCF-7 (IC_{50}, 7.09 ± 0.41) and HeLa (IC_{50}, 9.04 ± 0.34) cell lines. Additionally, *in silico* molecular docking was performed to study its binding interaction with *Mycobacterium tuberculosis* enoyl reductase (InhA) and drug-like features were studied using Swiss ADME tool. PASS analysis of all the compounds showed greater Pa than Pi value for the antituberculosis activity. The results suggested that the synthesized isoquinoline containing azo Schiff base derivatives becomes promising for developing new drugs to treat tuberculosis.

Keywords: Isoquinoline, Schiff derivatives, Antituberculosis activity, Cytotoxicity, Molecular docking, PASS prediction.

INTRODUCTION

Tuberculosis is a chronic bacterial contamination disease caused by an obligate bacterial pathogen *Mycobacterium tuberculosis* (MtB), which belongs to the family of *Mycobacteriaceae* [1] and primarily affects the lungs (Pulmonary TB). According to the World Health Organization's 2022 Global TB report, 10.6 million people were predicted to be infected with tuberculosis (TB) in 2021, an increase of 4.5% from 2020 and 1.6 million people died from TB including 0.187 million of HIV positive individuals [2]. A two-month intense phase of the drug susceptible (DS)-TB therapy with the first line drugs isoniazid (INH), rifampicin (RIF), pyrazinamide (PZA) and ethambutol (EMB) is followed by a continuation of the four-month phase of isoniazid and rifampicin [3]. Under optimal conditions, this medicine combination can cure 95% of DS-TB patients.

Treatment for multidrug resistant tuberculosis (MDR-TB) takes more than four years and includes second-line medica-

tions like kanamycin, capreomycin, fluoroquinolones, *etc*. In comparison to first-line medications, these drugs are more toxic, costly, limited and ineffective with greater adverse effects. Because of the COVID-19 pandemic in 2021, many TB services are disrupted and this is the first time in many years that an increase in the number of TB and drug-resistant TB cases has been reported. At the current state of improvement, low- and middle-income countries also continue to face the burden of communicable diseases, including TB, HIV and malaria will not meet their sustainable development goal targets by 2030. As a reference standard for interpreting mutations conferring resistance to all first line and a variety of second line TB drug(s), WHO released a report in June 2021 summarizing the analysis of over 38,000 isolates from more than 40 countries, with matched data on whole genome sequencing and phenotypic drug susceptibility testing for thirteen anti-TB medicines [4]. Involvement and innovative approaches are much needed to develop safer TB drug regimens against drug-resistant diseases.

Azo compounds with azo bond separated by two phenyl rings and azo-Schiff base derivatives are a very important class of organic compounds in the research area and known for their medicinal and pharmaceutical fields [5] and include biological activities such as antibacterial [6], anticancer [7], antifungal [8], antitubercular [9] and herbicidal activities [10]. Azo compounds are widely used substances in the paper, textile and colouring agents for foods and cosmetics industries [11,12]. In addition, isoquinoline derivatives are important heterocyclic compounds because of their broad existence in nature [13,14] and their pharmacological activities including antifungal [15], antibacterial [16], antitumor [17], anti-inflammatory [18], anti-convulsant [19], analgesic [20], antitubercular [21] and anti-cancer activities [22]. Keeping in mind of these views, the authors carried out the incorporation of isoquinoline moiety in the synthesis of novel and effective azo-Schiff derivatives and also evaluated for *in vitro* antitubercular activity and cyto-toxicity. *In silico* studies involving molecular docking, PASS prediction and ADME (absorption, distribution, metabolism, distribution) studies were performed for the synthesized compounds to check the possible binding interaction of the target protein with the ligand and to predict the drug likeness properties.

EXPERIMENTAL

Chemicals used for the synthesis were purchased from Sigma-Aldrich, USA. Solvents were purchased from SD Fine chemicals, India and used without further purification. Melting points of the product were established using an open capillary and are uncorrected. The progress of the reaction was moni-tored by TLC using Merck silica gel 60 F_{254} coated aluminum sheets and the developed spots were visualized by the ultra-violet light of 254 nm. The FT-IR spectra were recorded using Perkin-Elmer 1650 spectrometer by KBr disc method. ^{1}H NMR and ^{13}C NMR spectra were recorded at 400 MHz on JEOL JNM-ECZS instrument using DMSO-d_6 as solvent and tetra-methylsilane (TMS) as an internal standard. Mass spectra of the samples were recorded on Waters Alliance Micromass ZQ 2000LCMS and ESI-MS (*m/z*) values are given.

General method for the synthesis of compounds 2a-b: The new azo Schiff derivatives (**Scheme-I**) were synthesized according to the known procedure [23]. A diazonium solution was prepared by dissolving 5-aminoisoquinoline (1 mmol) in 10 mL of distilled water and 2 mL of conc. HCl and subjected to continuous stirring. To this solution, 1 mmol of $NaNO_2$ in 5 mL of ice-cold water was added dropwise and the reaction mixture was continued to stirred for 30 min by maintaining the temperature 0-5 ºC and then it was allowed to stand for 20 min to complete the diazotization reaction. Then, the diazonium solution was added slowly to the stirring solution of 1 mmol aniline (for **2a**)/*o*-toluidine (for **2b**) in 10 mL of ethanol and maintaining the reaction temperature of about 0 ºC. An orange-red precipitate was observed, which indicated the formation of azo compound. This mixture was then neutralized by adding Na_2CO_3 to maintain pH at 5-6 and allowed to stand overnight. The coloured precipitate obtained was filtered, washed with water and dried. The crude product was purified by repeated recrystallization using hot 95% ethanol. Intermediate compound **2a** yielded 80% with melting point 200-202 ºC, while compound **2b** yielded 85% with melting point 230-232 ºC.

General method for the synthesis of compounds 3a-f, 3g-l: Substituted aldehyde (1 mmol) in 5 mL of ethanol was stirred with 1 mmol of synthesized pure azo compound **2a** (for **3a-f**) or **2b** (for **3g-l**). Three drops of glacial acetic acid were added to the reaction mixture and refluxed for 8 h. The reaction was monitored by thin layer chromatography. The excess solvent from the reaction mixture was removed under pressure using a rotatory evaporator to get the solid and was washed with water and dried. The solid products **3a-f** and **3g-l** were recrystallized from hot ethanol.

N-(4-((*E*)-Isoquinolin-5-yldiazenyl)phenyl)-1-phenyl-methanimine (3a): Dark brown solid; yield: 88%; m.p.: 185-187 ºC; FT-IR (KBr, ν_{max}, cm^{-1}): 3139.2 (C-H, arom.), 1684.1 (C=N), 1581.6 (C=C), 1558.8 (C=C), 1498.3 (N=N), 1379.3 (C-N); ^{1}H NMR (400 MHz, DMSO-d_6) δ ppm: 7.02-8.77 (m, 14H, ArH), 9.44 (s, 1H, HC=N), 10.33 (s, 1H, CH-isoquino-line); ^{13}C NMR (400 MHz, DMSO-d_6) δ ppm: 110.0, 115.3, 115.7, 116.0, 116.5, 123.5, 126.4, 127.4, 128.5, 129.2, 129.7, 130.2, 131.2, 132.6, 136.2, 136.7, 141.5, 143.4, 148.1, 149.0, 150.6, 152.4; ESI-MS (*m/z*) calculated for $C_{22}H_{16}N_4$ [M+H]$^+$: 336.40, found: 337.38.

4-(((4-((*E*)-Isoquinolin-5-yldiazenyl)phenyl)imino)-methyl)phenol (3b): Dark brown solid; yield: 82%; m.p.: 170-172 ºC; FT-IR (KBr, ν_{max}, cm^{-1}): 3325.2 (O-H), 3129.5 (C-H, arom.), 1683.4 (C=N), 1599.4 (C=C), 1581.1 (C=C), 1498.9 (N=N), 1379.7 (C-N); ^{1}H NMR (500 MHz, DMSO-d_6) δ ppm: 7.01-8.71 (m, 13H, ArH), 9.40 (d, *J* = 28 Hz, 1H, CH-isoquino-line), 9.77 (s, 1H, HC=N), 10.22 (s, 1H, CH-isoquinoline), 10.32 (s, 1H, -OH); ^{13}C NMR (400 MHz, DMSO-d_6) δ ppm: 110.5, 115.3, 115.9, 116.4, 166.8, 123.2, 126.6, 127.5, 128.4, 129.7, 130.2, 131.6, 132.4, 136.9, 138.2, 141.6, 143.4, 147.9, 148.9, 151.5, 161.0, 163.4; ESI-MS (*m/z*) calculated for $C_{22}H_{16}N_4O$ [M+H]$^+$: 352.40, found: 353.18.

1-(4-Chlorophenyl)-N-(4-((*E*)-isoquinolin-5-yldiazenyl)-phenyl)methanimine (3c): Dark brown solid; yield: 83%; m.p.: 200-202 ºC; FT-IR (KBr, ν_{max}, cm^{-1}): 3119.6 (C-H, arom.), 1681.9 (C=N), 1620.7 (C=C), 1580.7 (C=C), 1497.7 (N=N), 1378.8 (C-N); ^{1}H NMR (500 MHz, DMSO-d_6) δ ppm: 7.00-8.77 (m, 12H, ArH), 9.40 (d, *J* = 27.2 Hz, 1H, CH-isoquino-line), 9.72 (s, 1H, HC=N), 10.32 (s, 1H, CH-isoquinoline); ^{13}C NMR (400 MHz, DMSO-d_6) δ ppm: 110.2, 115.4, 115.9, 116.4, 116.8, 117.4, 123.6, 126.7, 127.5, 129.2, 129.7, 130.2, 131.6, 134.5, 136.6, 143.4, 147.9, 148.6, 150.2, 151.4, 152.5, 160.0; ESI-MS (*m/z*) calculated for $C_{22}H_{15}ClN_4$ [M+H]$^+$: 370.84, found: 371.15.

N-(4-((*E*)-Isoquinolin-5-yldiazenyl)phenyl)-1-(4-methoxyphenyl)methanimine (3d): Dark brown solid; yield: 90%; m.p.: 213-215 ºC; FT-IR (KBr, ν_{max}, cm^{-1}): 3019.2 (C-H, arom.), 1682.8 (C=N), 1601.8 (C=C), 1512.2 (C=C), 1463.4 (N=N), 1380.6 (C-N); ^{1}H NMR (500 MHz, DMSO-d_6) δ ppm: 3.84 (s, 3H, OCH$_3$), 7.01-8.70 (m, 12H, ArH), 9.39 (d, *J* = 26.4 Hz, 1H, CH-isoquinoline), 9.85 (s, 1H, HC=N), 10.32 (s, 1H, CH-isoquinoline); ^{13}C NMR (400 MHz, DMSO-d_6) δ ppm: 55.6, 110.1, 115.2, 115.6, 115.8, 116.9, 120.8, 122.1, 123.5,
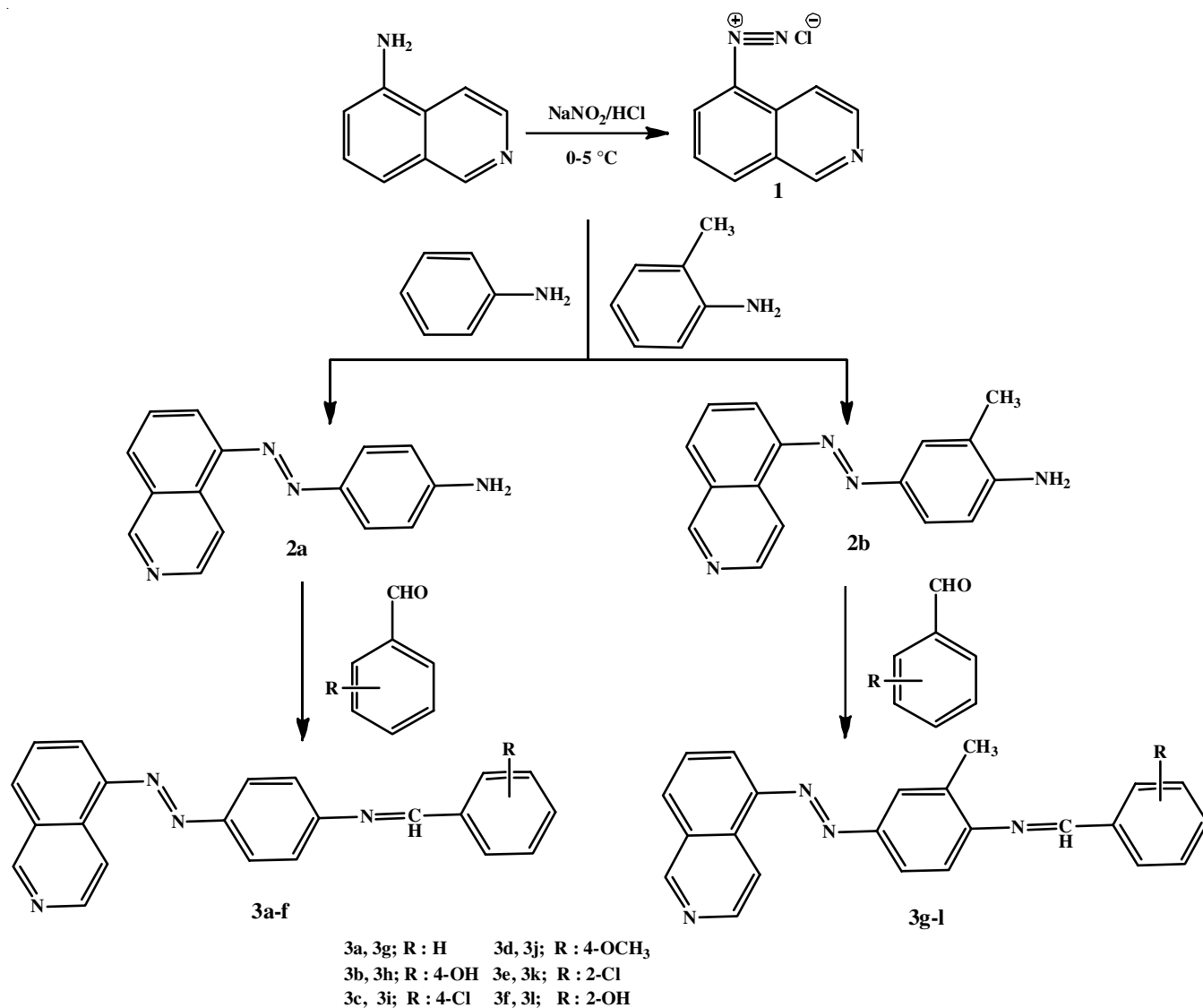
Scheme-I: Synthesis of isoquinolin-5-yldiazenyl)phenyl derivatives **3a-f** and **3g-l**

3a, 3g; R : H   3d, 3j; R : 4-OCH₃
3b, 3h; R : 4-OH   3e, 3k; R : 2-Cl
3c, 3i; R : 4-Cl   3f, 3l; R : 2-OH

125.4, 127.6, 128.9, 129.7, 130.8, 131.7, 141.8, 143.4, 148.2, 149.1, 151.7, 152.5, 159.8, 164.1; ESI-MS (*m/z*) calculated for $C_{23}H_{18}ON_4$ [M+H]⁺: 366.42, found: 367.19.

1-(2-Chlorophenyl)-*N*-(4-((*E*)-isoquinolin-5-yldiazenyl)-phenyl)methanimine (3e): Dark brown solid; yield: 89%; m.p.: 208-210 °C; FT-IR (KBr, ν_{max}, cm⁻¹): 3121.1 (C-H, arom.), 1681.0 (C=N), 1581.0 (C=C), 1497.1 (N=N), 1379.2 (C-N); ¹H NMR (500 MHz, DMSO-*d₆*) δ ppm: 7.27-8.85 (m, 12H, ArH), 9.41 (d, *J* = 13.6 Hz, 1H, CH-isoquinoline) 9.70 (s, 1H, HC=N), 10.33 (s, 1H, CH-isoquinoline); ¹³C NMR (400 MHz, DMSO-*d₆*) δ ppm: 115.1, 115.6, 115.9, 116.9, 120.9, 123.1, 126.5, 127.8, 128.3, 129.5, 130.1, 130.6, 132.5, 132.9, 134.9, 135.7, 136.2, 143.4, 148.3, 151.1, 152.5, 156.3; ESI-MS (*m/z*) calculated for $C_{22}H_{15}ClN_4$ [M+H]⁺: 370.84, found: 371.14.

2-(((4-((*E*)-Isoquinolin-5-yldiazenyl)phenyl)imino)-methyl)phenol (3f): Dark brown solid; yield: 84%; m.p.: 231-233 °C; FT-IR (KBr, ν_{max}, cm⁻¹): 3315.4 (O-H), 3118.2 (C-H, arom.), 1683.6 (C=N), 1652.7 (C=C), 1580.9 (C=C), 1497.6 (N=N), 1378.7 (C-N); ¹H NMR (500 MHz, DMSO-*d₆*) δ ppm:

7.01-8.98 (m, 12H, ArH), 9.37 (d, *J* = 38.0 Hz, 1H, CH-iso-quinoline), 10.31 (s, 1H, HC=N), 10.68 (s, 1H, CH-isoquino-line), 12.36 (s, 1H, OH); ¹³C NMR (400 MHz, DMSO-*d₆*) δ ppm: 110.3, 115.5, 115.8, 116.2, 116.6, 123.5, 126.4, 127.9, 128.42, 129.4, 130.7, 131.1, 132.2, 135.2, 135.2, 136.8, 141.2, 143.3, 148.0, 149.2, 150.6, 160.2, 164.1; ESI-MS (*m/z*) calculated for $C_{22}H_{16}N_4O$ [M+H]⁺: 352.40, found: 353.42.

N-(4-((*E*)-Isoquinolin-5-yldiazenyl)-2-methylphenyl)-1-phenylmethanimine (3g): Dark brown solid; yield: 83%; m.p.: 197-199 °C; FT-IR (KBr, ν_{max}, cm⁻¹): 3023.4 (C-H, arom.), 1692.0 (C=N), 1581.1 (C=C), 1553.7 (C=C), 1462.1 (N=N), 1379.3 (C-N); ¹H NMR (500 MHz, DMSO-*d₆*) δ ppm: 2.67 (s, 3H, CH₃), 7.01-8.72 (m, 12H, ArH), 9.41 (d, *J* = 13.2 Hz, 1H, CH-isoquinoline), 9.73 (s, 1H, HC=N), 10.32 (s, 1H, CH-isoquinoline); ¹³C NMR (400 MHz, DMSO-*d₆*) δ ppm: 17.3, 110.1, 115.3, 115.9, 116.3, 123.5, 126.5, 127.7, 128.5, 129.2, 129.6, 130.7, 131.1, 132.8, 136.4, 136.8, 141.6, 143.3, 148.2, 148.9, 150.7, 152.5, 160.3; ESI-MS (*m/z*) calculated for $C_{23}H_{18}N_4$ [M+H]⁺: 350.42, found: 351.20.

4-(((4-((*E*)-Isoquinolin-5-yldiazenyl)-2-methylphenyl)-imino)methyl)phenol (3h): Dark brown solid; Yield: 88%; m.p.: 181-183 ℃; FT-IR (KBr, v_{max}, cm^{-1}): 3328.3 (O-H), 3126.9 (C-H, arom.), 1682.4 (C=N), 1597.8 (C=C), 1581.2 (C=C), 1499.2 (N=N), 1379.1 (C-N); ^{1}H NMR (500 MHz, DMSO-d_6) δ ppm: 2.67 (s, 3H, CH$_3$), 6.90-8.70 (m, 11H, ArH), 9.37 (d, *J* = 14.0 Hz, 1H, CH-isoquinoline), 9.77 (s, 1H, HC=N), 10.22 (s, 1H, CH-isoquinoline), 10.32 (s, 1H, OH); ^{13}C NMR (400 MHz, DMSO-d_6) δ ppm: 17.3, 110.2, 115.1, 115.8, 116.0, 116.9, 123.6, 126.5, 127.8, 128.2, 129.5, 130.18, 131.5, 132.1, 136.5, 137.9, 141.7, 143.2, 148.1, 148.6, 150.9, 161.2, 163.1; ESI-MS (*m/z*) calculated for C$_{23}$H$_{18}$ON$_4$ [M+H]$^+$: 366.42, found: 367.19.

1-(4-Chlorophenyl)-*N*-(4-((*E*)-isoquinolin-5-yldiazenyl)-2-methylphenyl)methanimine (3i): Dark brown solid; yield: 91%; m.p.: 176-178 ℃; FT-IR (KBr, v_{max}, cm^{-1}): 3125.9 (C-H, arom.), 1682.0 (C=N), 1621.2 (C=C), 1581.2 (C=C), 1497.5 (N=N), 1378.4 (C-N); ^{1}H NMR (500 MHz, DMSO-d_6) δ ppm: 2.68 (s, 3H, CH$_3$), 7.01-8.74 (m, 11H, ArH), 9.40 (d, *J* = 28.0 Hz, 1H, CH-isoquinoline), 9.71 (s, 1H, HC=N), 10.33 (s, 1H, CH-isoquinoline); ^{13}C NMR (400 MHz, DMSO-d_6) δ ppm: 17.3, 110.2, 115.2, 115.3, 116.0, 116.5, 117.0, 123.5, 126.6, 127.8, 128.7, 129.1, 131.2, 132.9, 134.5, 136.5, 143.5, 148.3, 149.0, 150.1, 151.0, 152.4, 159.0; ESI-MS (*m/z*) calculated for C$_{23}$H$_{17}$ClN$_4$ [M+H]$^+$: 384.87, found: 385.16.

N-(4-((*E*)-Isoquinolin-5-yldiazenyl)-2-methylphenyl)-1-(4-methoxyphenyl)methanimine (3j): Dark brown solid; yield: 90%; m.p.: 220-222 ℃; FT-IR (KBr, v_{max}, cm^{-1}): 3119.7 (C-H, arom.), 1679.9 (C=N), 1605.7 (C=C), 1579.3 (C=C), 1461.9 (N=N), 1377.2 (C-N); ^{1}H NMR (500 MHz, DMSO-d_6) δ ppm: 2.68 (s, 3H, CH$_3$), 3.85 (s, 3H, OCH$_3$), 7.04-8.77 (m, 11H, ArH), 9.40 (d, *J* = 38.0 Hz, 1H, CH-isoquinoline), 9.73 (s, 1H, HC=N), 10.33 (s, 1H, CH-isoquinoline); ^{13}C NMR (400 MHz, DMSO-d_6) δ ppm: 17.3, 55.8, 110.3, 115.0, 115.9, 116.9, 118.3, 120.9, 122.5, 123.2, 125.8, 127.5, 128.7, 129.7, 130.8, 131.4, 141.2, 143.4, 150.2, 151.1, 152.5, 153.3, 160.0, 163.0; ESI-MS (*m/z*) calculated for C$_{24}$H$_{20}$ON$_4$ [M+H]$^+$: 380.45, found: 381.49.

1-(2-Chlorophenyl)-N-(4-((*E*)-isoquinolin-5-yldiazenyl)-2-methylphenyl)methanimine (3k): Dark brown solid; yield: 89%; m.p.: 204-206 ℃; FT-IR (KBr, v_{max}, cm^{-1}): 3019.9 (C-H, arom.), 1681.3 (C=N), 1597.8 (C=C), 1584.3 (C=C), 1499.2 (N=N), 1379.9 (C-N); ^{1}H NMR (500 MHz, DMSO-d_6) δ ppm: 2.67 (s, 3H, CH$_3$), 7.00-8.73 (m, 11H, ArH), 9.41 (d, *J* = 13.2 Hz, 1H, CH-isoquinoline), 9.78 (s, 1H, HC=N), 10.32 (s, 1H, CH-isoquinoline); ^{13}C NMR (400 MHz, DMSO-d_6) δ ppm: 17.2, 110.4, 115.3, 115.7, 116.2, 116.3, 117.9, 126.6, 127.7, 128.9, 129.1, 129.7, 130.7, 131.95, 133.6, 135.3, 137.8, 143.8, 145.3, 148.5, 149.6, 150.5, 158.6; ESI-MS (*m/z*) calculated for C$_{23}$H$_{17}$ClN$_4$ [M+H]$^+$: 384.87, found: 385.16.

2-(((4-((*E*)-Isoquinolin-5-yldiazenyl)-2-methylphenyl)-imino)methyl)phenol (3l): Dark brown solid; yield: 83%; m.p.: 225-227 ℃; FT-IR (KBr, v_{max}, cm^{-1}): 3320.2 (O-H), 3040.9 (C-H, arom.), 1611.6 (C=N), 1571.8 (C=C), 1556.7 (C=C), 1481.1 (N=N), 1376.9 (C-N); ^{1}H NMR (500 MHz, DMSO-d_6) δ ppm: 2.67 (s, 3H, CH$_3$), 7.00-9.08 (m, 11H, ArH), 9.40 (d, *J* = 22.4 Hz, 1H, CH-isoquinoline), 10.24 (s, 1H, HC=N), 10.70 (s, 1H, CH-isoquinoline), 12.34 (s, 1H, OH); ^{13}C NMR (400

MHz, DMSO-d_6) δ ppm: 17.3, 110.2, 115.3, 115.7, 116.4, 116.6, 123.6, 126.6, 127.7, 127.9, 129.2, 129.7, 131.2, 132.3, 136.4, 136.9, 141.4, 143.4, 148.2, 148.8, 150.7, 160.7, 164.6; ESI-MS (*m/z*) calculated for C$_{23}$H$_{18}$N$_4$O [M+H]$^+$: 366.42, found: 367.19.

Biological evaluation

***In vitro* antituberculosis activity:** The newly synthesized compounds (**3a-l**) were screened for anti-tubercular activity against *M. tuberculosis* H37Rv (MTB) for minimum inhibitory concentration determination (MIC) by using microplate alamar blue assay (MABA) method. To the outer perimeter of the sterile 96-well microtiter plate, 200 μL of sterile deionized water was added to decrease the evaporation and to maintain humidity of the medium in the test wells during incubation. The *M. tuberculosis* H37Rv strain was suspended in 100 μL of the Middlebrook 7H9 broth and each test sample stock solution was thawed and serial two-fold dilution was carried out directly on the plate and at 100 to 0.2 μg/mL, the final drug concentration was tested. Plates were sealed with parafilm and incubated at 37 ℃ for a week. After an incubation period, 25 μL of freshly prepared mixture of Alamar blue reagent and 10% Tween 80 were added to each well and the plate was re-incubated for 24 h. A blue colour solution in the well was considered as having no bacterial growth and pink colour indicated bacterial growth. The MIC value was noted for the lowest concentration of the drug at which, there was no change in colour observed from blue to pink indicated for the inhibition of the growth of bacteria. Each sample was tested in triplicates and isoniazid, rifampicin and ethambutol were used as positive control [24].

***In vitro* cytotoxicity screening:** The active compounds were screened for cell toxicity against two human cancer cell lines, MCF-7 (breast carcinoma) and HeLa (cervical carcinoma) by MTT (3-(4,5-dimethylthiazol-2-yl)-2,5-diphenyltetrazolium bromide) assay. Cells were seeded in 96-well micro-plate over-night with 95% humidity and 5% CO$_2$ at 37 ℃ in Dulbecco's Modified Eagle Media (DMEM) containing 10% heat inacti-vated fetal bovine serum (FBS) and 1% antibiotic-antimycotic solution. The cells were treated with different concentrations of the samples and incubated for another 48 h. The wells were washed twice with phosphate-buffered saline (PBS) and 20 μL of the MTT staining solution was added to each well and incubated for 4 h at 37 ℃. The formazan crystals thus formed were dissolved in 100 μL of DMSO and absorbance was recorded at 570 nm using the multimode reader. The percentage cell viability was calculated by using the given equation [25]:

$$\text{Cell viability (\%)} = \frac{\text{Optical density of test cells}}{\text{Optical density of control cells}} \times 100$$

The experimental conditions were carried out in three replicates and IC$_{50}$ of each compound was calculated using Graph Pad Prism program.

Computational studies

Molecular docking study: The 3D structures of the newly synthesized ligands (**3a-l**) were drawn in Chem Draw Ultra software. The crystal structure of the target protein *M. tuberculosis*

enoyl reductase (INHA)) was retrieved from the RCSB protein databank (http://www.rcsb.org) as a PDB file with the PDB ID: 4TZK, resolution 1.62 Å. The docking of the ligand and the chosen receptor was carried out with the help of Auto Dock tools 1.5.6. software installed in a windows 10 operating system. Molecular docking includes the first step as the preparation of ligands and receptors according to the input criteria before the analysis. Initially, protein structure was prepared by removing all water molecules and hetero atoms followed by the addition of polar hydrogen atoms, kollman charges and saved in PDBQT format. Further ligand structure was prepared by adding hydrogen atoms and gasteiger charges individually and were processed in PDBQT file format as the input file for docking in Auto dock tools. A three-dimensional grid box was generated to identify the XYZ coordinates around the binding site of the enzyme and the parameters were saved as config.file. The command prompt was run to get the output file of the docking score with 10 possible conformations [26]. Among the obtained conformers, the least docked energy structure was selected to study the binding interaction with the protein using Discovery Studio Visualizer.

ADME prediction method: The synthesized compounds (**3a-l**) were studied for their physico-chemical, pharmaco-kinetic, drug-likeness and absorption properties [27,28]. Brain or intestinal estimated permeation (BOILED-Egg) indicates the estimation of passive gastrointestinal absorption and brain penetration [29]. Bioavailability radar was used to predict the drug-likeness of a molecule.

PASS analysis: *In silico* PASS prediction of the compounds (**3a-l**) were analyzed by the PASS (prediction of activity spectra for substance) for their antimycobacterial and antituberculosis activity along with the standard isoniazid using web portal http://www.way2drug.com/passonline/. The prediction of activity is based on structure-activity relationship analysis of the training set containing more than 35,000 compounds which have more than 4000 kinds of biological activity including pharmacological effects, mechanisms of action, toxic and adverse effects, interaction with metabolic enzymes and trans-porters, influence on gene expression, *etc.* with mean accuracy of prediction about 95% based on the compound's structural formula [30]. The result estimates predicted activity spectrum of a compound as probable activity (Pa) and probable inactivity (Pi). The activity of the compounds was considered only with Pa > Pi and the values of Pa and Pi lies between 0.000 and 1.000. If Pa > 0.7, the substance is very likely to exhibit the activity in experiment and possess high pharmacological action. If 0.5 < Pa < 0.7, probability of experimental pharmacological action is less. If Pa < 0.5, the substance might be a new chemical entity with less chance of finding the activity experimentally [31,32].

RESULTS AND DISCUSSION

The azo compounds (**2a-b**) were synthesized according to the reported procedure [33]. Diazonium salt was prepared by reacting nitrous acid with 5-aminoisoquinoline at 0-5 ºC. Then, the solution was diazotized with aniline to get 4-(isoqui-nolin-5-yldiazenyl)aniline (**2a**) and *o*-toluidine to afford 4-(isoquinolin-5-yldiazenyl)-2-methylaniline (**2b**). Azo Schiff base derivatives (**3a-l**) were then synthesized by the condensation reaction of synthesized azo isoquinoline amine intermediates (**2a-b**) with various substituted aromatic aldehyde in absolute ethanol (**Scheme-I**). The final compounds were purified by repeated crystallization using ethanol solvent. The products yields were obtained in the range from 82-91%. Sharp melting point of the title compounds were obtained and further confir-med through spectral characterization *viz*. FT-IR, ^{1}H NMR, ^{13}C NMR and mass spectroscopy. The synthesized compound **3a** showed an absorption band for C=N at 1684.1 cm^{-1}, C=C stretching frequency at 1558.8 cm^{-1} and N=N stretching frequency band at 1498.3 cm^{-1} in the respective IR spectrum. ^{1}H NMR chemical shift values (δ, ppm) of the same compound were assigned as 7.02-8.77 (m, 14H, ArH), 9.44 (s, 1H, HC=N) and 10.33 (s, 1H, CH-isoquinoline). ^{13}C NMR signals of compound **3a** were well correlated with its structure and mass analysis showed [M+H]$^+$ ion peak at *m/z* value 337.38, which is correla-ting with its molecular formula $C_{22}H_{16}N_4$.

Biological evaluation

***In vitro* antituberculosis activity:** *In vitro* antitubercular activity of the synthesized derivatives (**3a-l**) was carried out using the microplate alamar blue assay (MABA) method against *M. tuberculosis* H37Rv strain (ATCC No-27294). The standard drugs, isoniazid, pyrazinamide and ethambutol were included for comparison. The two series of azo Schiff compounds, *viz.* (4-((E)-isoquinolin-5-yldiazenyl)phenyl) derivatives (**3a-f**) and (4-((E)-isoquinolin-5-yldiazenyl)-2-methylphenyl) derivatives (**3g-l**) were showed variation in the anti-tubercular activity. The determined MIC values are reported in Table-1 and all the tested samples illustrated good to excellent anti-tuberculosis activity with MIC values ranging from 1.6 to 50 µg/mL. Among the compounds screened for their anti-tuberculosis properties, compound **3b** showed excellent activity with potency equal to standards, ethambutol and Isoniazid (MIC 1.6 µg/mL). The compounds **3a** and **3c** showed potential activity equal to that of pyrazinamide (MIC 3.125 µg/mL). Compound **3d** showed significant activity (MIC 6.25 µg/mL) and compounds **3f**, **3h**, **3i** and **3l** exhibited good activity with MIC 12.5 µg/mL. The plausible structure activity relationship can be drawn by corre-lating obtained MIC values of the synthesized compounds with their structures. From the *in vitro* results, it was observed that aniline moiety containing azo Schiff (4-(isoquinolin-5-yldia-zenyl)-2-methylphenyl) derivatives showed higher activity with low MIC values when compared to that of toluidine moiety containing azo Schiff (4-((E)-isoquinolin-5-yldiazenyl)-2-methylphenyl) derivatives. The target compounds have either electron withdrawing group -Cl or electron donating (OH and OCH$_3$) groups substitution at *ortho* or *para* position of the phenyl ring of aldehyde moiety besides diazyl isoquinoline core structure. It was observed that isoquinoline ring containing azo Schiff derivatives with various substitutions at *para* position (**3b**, **3c** and **3d**) and unsubstituted compound **3a** showed better activity over the *ortho* (**3f**, **3l** and **3k**) substituted derivatives. The presence of the methyl group at C2 position of the phenyl

TABLE-1
MIC VALUES, BINDING SCORE AND INTERACTED AMINO ACID
RESIDUES OF THE TARGET PROTEIN FOR THE TITLE COMPOUNDS (3a-l)

Compound	R	MIC (μg/mL)[a]	Binding score (kcal/mol)	Interacted amino acid residue
3a	H	3.125	-7.6	Ala128, Val171, Lys132
3b	4-OH	1.600	-8.1	Ala128, Val171, Phe174, Val175, Lys132, Tyr 182
3c	4-Cl	3.125	-7.9	Ala128, Ala131, Lys132, Ala167, Val171, Phe174, Val175
3d	4-OCH₃	6.250	-7.6	Ala128, Ala131, Lys132, Ala167, Val171, Phe174, Val175
3e	2-Cl	50.000	-8.1	Ala128, Lys132, Val171, Val174, Val175
3f	2-OH	12.500	-8.1	Ala128, Lys132, Leu135, Val171, Phe174, Val175
3g	H	50.000	-8.3	Ala128, Lys132, Val171, Val175, Phe174
3h	4-OH	12.500	-8.3	Ala128, Lys132, Val171, Val175, Tyr182
3i	4-Cl	12.500	-8.4	Ala128, Lys132, Val171, Val175, Phe174
3j	4-OCH₃	50.000	-7.8	Ala128, Ala131, Lys132, Leu135, Pro136, Ala167, Val171, Glu178, Tyr182
3k	2-Cl	25.000	-8.4	Ala128, Lys132, Val171, Phe174, Val175
3l	2-OH	12.500	-8.4	Ala128, Lys132, Leu135, Val171, Phe174, Val175
Isoniazid[b]		1.600	-5.8	
Pyrazinamide[b]		3.125	-8.1	
Ethambutol[b]		1.600	-4.5	

[a]MIC was determined with a drug concentration from 100 μg/mL to 0.8 μg/mL; [b]Reference standard

ring attached to azo group and the various substitution on the other phenyl ring derivatives (**3e**, **3g** and **3j**) exhibited moderate activity. The overall analysis summarizes isoquinoline containing azo Schiff base derivatives could be considered as a precursor structure for the further development of anti-tubercular drugs.

Cytotoxicity assay: Among the tested compounds, four major compounds (**3a-l**) showed the highest anti-tubercular activity with low MIC values, were further evaluated for their cytotoxic properties using MTT (3-(4,5-dimethylthiazol-2-yl)-2,5-diphenyltetrazolium bromide) assay against MCF-7 (breast) and HeLa (cervical) cell lines using doxorubicin (DOX) as a reference standard and their IC_{50} values are given in Table-2. After 48 h of exposure and based on the conversion of MTT into the formazan product the viability of the cells was assessed and the graph of their values at different concentrations is plotted as shown in Fig. 1. The current study indicated that compound **3b** possessed the highest cytotoxic activity against MCF-7 (IC_{50}, 7.09 ± 0.41) and HeLa (IC_{50}, 9.04 ± 0.34) cell lines. Among the tested compounds, comparably less activity was exhibited with **3a** against MCF-7 (IC_{50}, 15.16 ± 0.82) and

TABLE-2
In vitro CYTOTOXIC ACTIVITY OF **3a-d** COMPOUNDS
AGAINST MCF-7 AND HeLa CELL LINES

Compounds	IC_{50} (μM)	
	MCF-7	Hela
3a	15.16 ± 0.82	12.88 ± 0.51
3b	7.09 ± 0.41	9.04 ± 0.34
3c	10.06 ± 0.52	16.84 ± 0.20
3d	11.14 ± 0.61	17.44 ± 0.09
Doxorubicin	1.75 ± 0.05	1.75 ± 0.05

Values are expressed as mean ± standard deviation of triplicate determinations

with **3d** against HeLa (IC_{50}, 17.44 ± 0.09) cell line. The analysis indicated that the substitution of electron donating group -OH at *para* position of (4-((*E*)-isoquinolin-5-yldiazenyl)phenyl) moiety made an effective impact on exhibiting potential activity.

Computational studies

Molecular docking study: A molecular docking study was carried out to know the probable binding interactions of
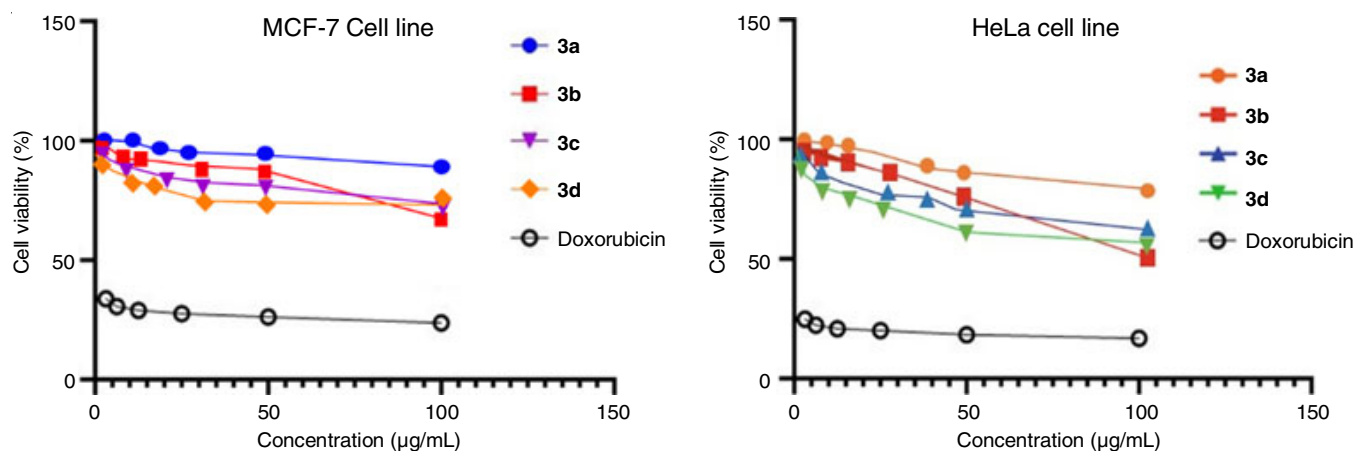

Fig. 1. Graph representing % cell viability *vs.* concentration for the evaluation of cytotoxicity against MCF-7 and HeLa cell lines using MTT assay

the synthesized ligand (**3a-l**) with the target protein PDB code: 4TZK and X-ray resolution 1.62 Å against *M. tuberculosis* enoyl reductase (InhA). All the molecules exhibited binding energies in the range of -7.6 to -8.4 kcal/mol and the values are given in Table-1. Isoniazid, ethambutol and pyrazinamide were used as reference standard with binding scores -5.8, -4.5

and -8.1 kcal/mol, respectively. Compounds **3i, 3k** and **3l** showed the highest docking score of -8.4 kcal/mol, whereas compound **3b** showed excellent *in vitro* antitubercular activity equivalent to that of standard reference isoniazid and ethambutol with docking score -8.1 kcal/mol and the amino acid residues involved in the binding interactions are Ala128, Val171, Phe174,
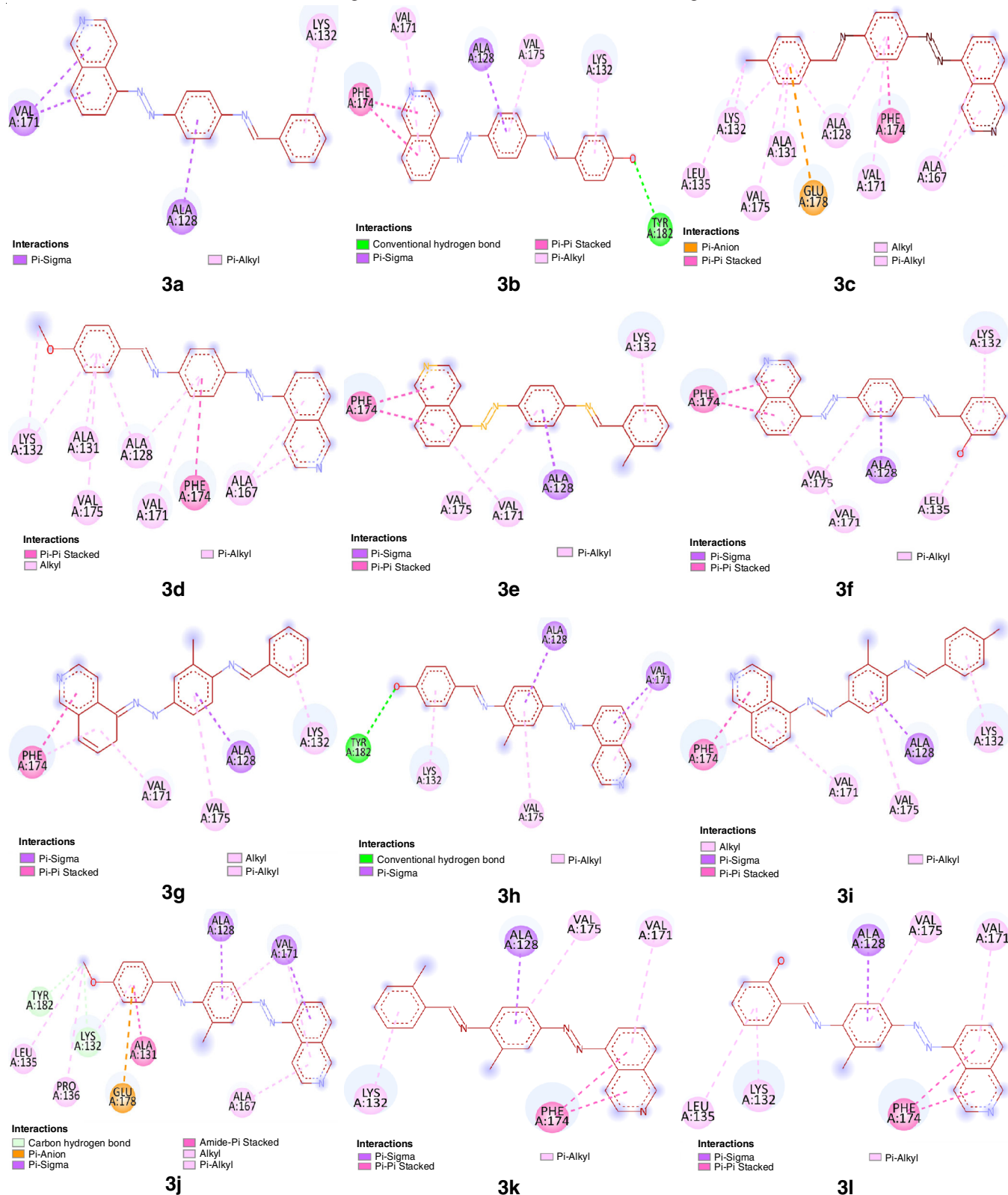
Fig. 2. Interaction of synthesized ligand (**3a-l**) with protein InhA (PDB: 4TZK) representation in 2D

Val175, Lys132 and Tyr 182. All the compounds exhibited negative binding scores indicating the stability of the compounds. The prominent binding interactions involved are pi-sigma, pi-alkyl, pi-anion, pi-pi stacked, alkyl, amide-pi stacked. Along with these interactions, the hydrogen bond involved in compounds **3b**, **3h** and **3j** indicates more stability of the complex and facilitates the accuracy of binding energy calculation. Visualization of the binding interactions in 2D and 3D format obtained from discovery studio software is shown in Figs. 2 and 3.
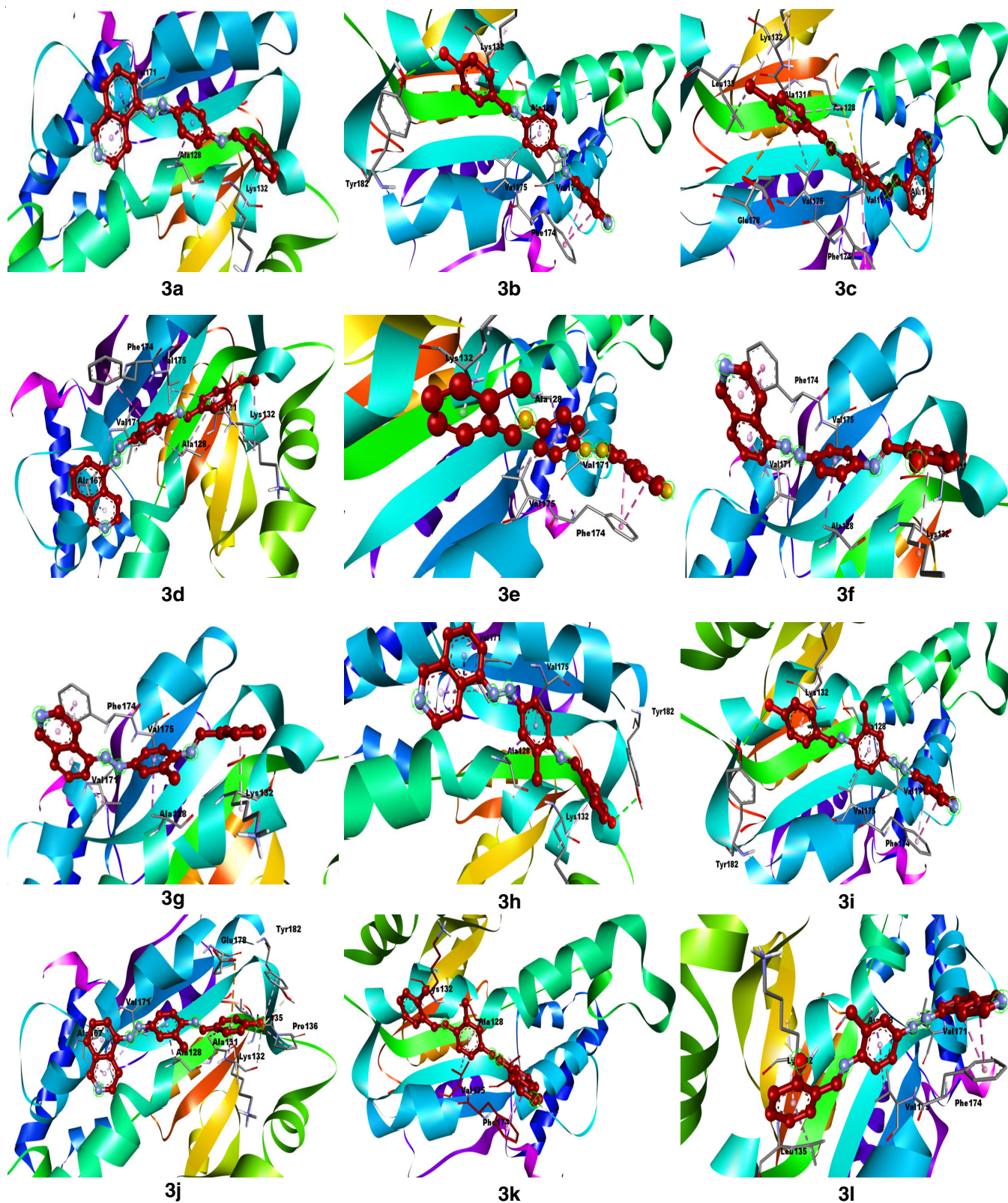
Fig. 3. Interaction of synthesized ligand (**3a-l**) with protein InhA (PDB: 4TZK) representation in 3D

Prediction of *in silico* ADME properties: All the molecules showed excellent physico-chemical parameters (Table-3) and obeyed Lipinski's rule of five. It is a thumb rule for evaluating drug-likeness and states that a molecule or an inhibitor with a certain biological and pharmacological property would be orally active if two or more of these criteria are not violated (*m.w.* ≤ 500 amu, Log P ≤ 5, hydrogen bond donor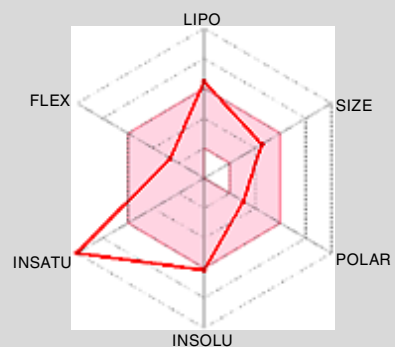s ≤ 5, hydrogen bond acceptor ≤ 10, number of rotatable bonds ≤ 10, molar refractivity ≤ 130, tropological polar surface area ≤ 140) [34,35].

The BOILED-Egg representation indicates the evaluation of passive gastrointestinal absorption (HIA) and brain penetration (BBB) in the function of the position of the molecules in the WLOGP on *y*-axis *versus* TPSA on *x*-axis referential. According to this predictive model if a molecule falls in the white region represents a high probability of passive absor-
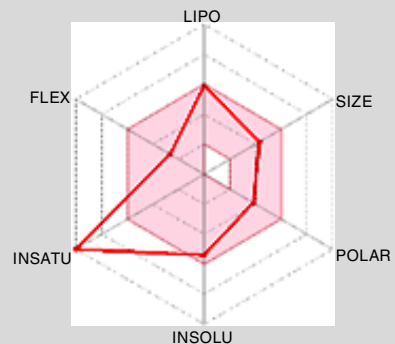
TABLE-3 *In silico* ADME PROPERTIES OF THE COMPOUNDS **3a-l**									
Comp.	MW	FC	NRB	NHA	NHD	MR	TPSA	iLog P	BS	BAR
3a	336.39	0.00	4	4	0	106.06	49.97	3.60	0.55	
3b	352.39	0.00	4	5	1	108.08	70.20	3.24	0.55	
3c	370.83	0.00	4	4	0	111.07	49.97	3.87	0.55	
3d	366.42	0.04	5	5	0	112.55	59.20	3.86	0.55	

3e	370.83	0.00	4	4	0	111.07	49.97	3.89	0.55
3f	352.39	0.00	4	5	1	108.80	70.20	3.28	0.55
3g	350.42	0.04	4	4	0	111.02	49.97	3.88	0.55
3h	366.42	0.04	4	5	1	113.05	70.20	3.51	0.55
3i	384.86	0.04	4	4	2	116.03	49.97	4.08	0.55
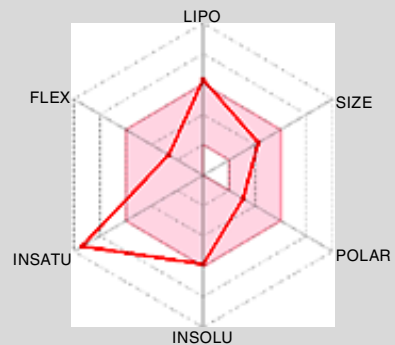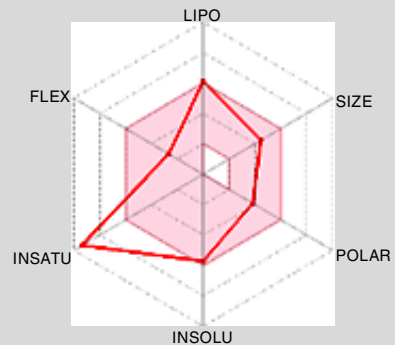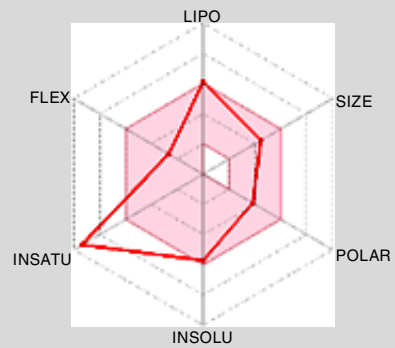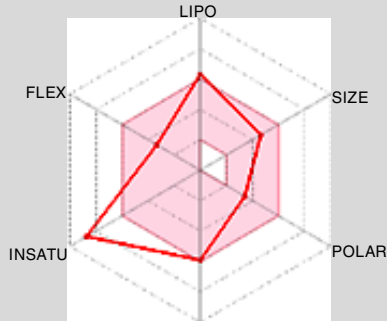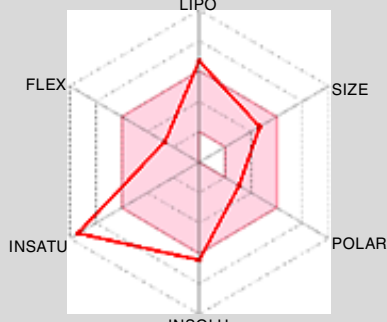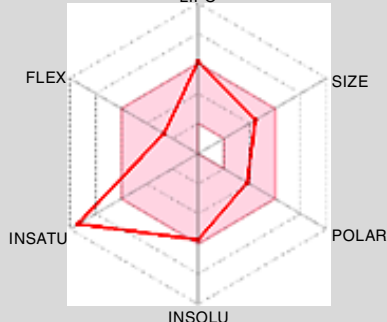
Compound	MW	FC	NRB	NHA	NHD	MR	TPSA	iLog P	BS	BAR
3j	380.44	0.08	5	5	0	117.52	59.20	4.17	0.55	
3k	384.86	0.04	4	4	0	116.03	49.97	4.11	0.55	
3l	366.42	0.04	4	5	1	113.05	70.20	3.52	0.55	
Isoniazid	137.14	0.00	2	3	2	35.13	68.01	0.03	0.55	

MW: Molecular weight (g/mol), FC: Fraction CSP^3, NRB: Number of rotatable bonds, NHA: Number of hydrogen acceptor, NHD: Number of hydrogen donar, MR: Molar refractivity; TPSA: Tropological surface area, iLog P: Octanol/water partition coefficient, BS: Bioavailability score, BAR: Bioavailability radar.

ption by the gastrointestinal tract, the yellow region (yolk) is for the high probability of brain penetration and the blue point is predicted as actively effluxed by permeability glycoprotein (PGP+) and red point represents as non-substrate of (PGP-). From the Boiled egg graph (Fig. 4), it is observed that compounds **3d, 3e, 3i** and **3k** are not absorbed and not brain penetrant (outside egg) and the other compounds lying in the white region are well absorbed but not accessing the brain. Drug likeness assesses the qualitative possibility for a molecule to become an oral drug and the pink area of the radar (Table-3) signifies the optimum physicochemical space for each property in all the compounds predicted to be orally bioavailable with the bioactivity score of 0.55. All the synthesized derivatives showed good physico-chemical properties, which are infusing the good ADME properties.

PASS prediction: The results of the analyzed compounds for the activities of antimycobacterial and antituberculosis as Pa and Pi are expressed in Table-4. All the synthesized derivatives (**3a-l**) showed greater Pa than Pi. Pass prediction of the
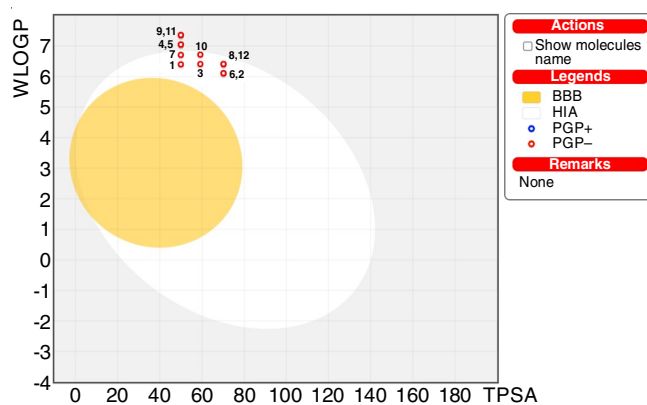

Fig. 4.　BOILED-egg graph representation of the synthesized compounds for the evaluation of passive gastrointestinal absorption (HIA) and brain penetration (BBB). In this figure numerical numbers from 1 to 12 sequentially represent the title compounds **3a-l**

compounds were found to be as 0.46 < Pa < 0.69 in antimycobacterial activity and 0.49 < Pa < 0.74 in antituberculosis

Compound	Antimycobacterial		Antituberculosis	
	Pa	Pi	Pa	Pi
3a	0.653	0.007	0.695	0.004
3b	0.666	0.006	0.717	0.004
3c	0.646	0.008	0.673	0.004
3d	0.656	0.007	0.674	0.004
3e	0.528	0.015	0.557	0.008
3f	0.691	0.005	0.746	0.004
3g	0.591	0.010	0.633	0.005
3h	0.610	0.009	0.659	0.005
3i	0.579	0.011	0.605	0.005
3j	0.597	0.010	0.606	0.005
3k	0.465	0.025	0.494	0.013
3l	0.640	0.008	0.689	0.004
Isoniazid	0.798	0.004	0.810	0.003

TABLE-4. PASS ANALYSIS RESULTS OF THE COMPOUNDS 3a-l

activity, it was compared with the standard isoniazid whose Pa is 0.79 in antimycobacterial activity and 0.81 in antituberculosis activity. Compound **3f** showed the highest Pa value in both the activities among other compounds. The significant results revealed that these compounds are new chemical entities which could act as potent antituberculosis agents.

Conclusion

A series of isoquinoline containing azo Schiff base derivatives were synthesized, characterized and evaluated for their *in vitro* antituberculosis activity by MABA method and cytotoxicity using MTT assay. The results revealed that compound **3b** was found to be a potent antitubercular agent with the lowest MIC value of 1.6 µg/mL against *M. tuberculosis* H37Rv strain. The activity of compound **3b** has been comparable with that of reference standard and therefore it could become promising antitubercular agent. Further compound **3b** showed the highest cytotoxicity against MCF-7 (IC_{50}, 7.09 ± 0.41) and HeLa (IC_{50}, 9.04 ± 0.34) cell lines. Other compounds of the series showed good to moderate activity. Additionally, *in silico* molecular docking and drug likeness properties were studied, which support the current results. The title compounds displayed a negative binding score in docking, indicating the stability of the complex and exhibiting the various binding interactions in the active region. Compounds showed good adsorption, distribution, metabolism and excretion (ADME) properties without Lipinski's violation, which is desirable for the oral absorption of drug candidates. Computational studies revealed that the tested compounds are safe with druggable properties and acceptable ADME properties. Therefore, the synthesized isoquinoline containing azo Schiff base derivatives could be considered as a precursor structure for the development of potential drugs against tuberculosis.

CONFLICT OF INTEREST

The authors declare that there is no conflict of interests regarding the publication of this article.

REFERENCES

1. N.R. Gandhi, A. Moll, A.W. Sturm, R. Pawinski, T. Govender, U. Lalloo, K. Zeller, J. Andrews and G. Friedland, *Lancet*, **368**, 1575 (2006); https://doi.org/10.1016/S0140-6736(06)69573-1
2. World Health Organization, Rapid communication: Key Changes to the Treatment of Drug-Resistant Tuberculosis, Global Tuberculosis Report, Geneva (2022).
3. R. Johnson, E.M. Streicher, G.E. Louw, R.M. Warren, P.D. Van Helden and T.C. Victor, *Curr. Issues Mol. Biol.*, **8**, 97 (2006).
4. World Health Organization, Catalogue of Mutations in *Mycobacterium tuberculosis* Complex and their Association with Drug Resistance, Global Tuberculosis Report, Geneva (2021).
5. K. Mezgebe and E. Mulugeta, *RSC Adv.*, **12**, 25932 (2022); https://doi.org/10.1039/d2ra04934a
6. A. Naqvi, M. Shahnawaaz, A.V. Rao, D.S. Seth and N.K. Sharma, *E-J. Chem.*, **6(s1)**, S75 (2009); https://doi.org/10.1155/2009/589430
7. H. Luo, Y. Xia, B. Sun, L. Huang, X. Wang, H.-y. Lou, X. Zhu, W. Pan and X. Zhang, *Biochem. Res. Int.*, **2017**, 6257240 (2017); https://doi.org/10.1155/2017/6257240
8. H. Xu and X. Zeng, *Bioorg. Med. Chem. Lett.*, **20**, 4193 (2010); https://doi.org/10.1016/j.bmcl.2010.05.048
9. G. More, S. Bootwala, S. Shenoy, J. Mascarenhas and K. Aruna, *Int. J. Pharma Sci.*, **9**, 3029 (2018); https://doi.org/10.13040/IJPSR.0975-8232.9(7).3029-35
10. S. Samadhiya and A. Halve, *Orient. J. Chem.*, **17**, 119 (2001).
11. F. Hamon, F. Djedaini-Pilard, F. Barbot and C. Len, *Tetrahedron*, **65**, 10105 (2009); https://doi.org/10.1016/j.tet.2009.08.063
12. P. Gordon, Nontextile Applications of Dyes, In: The Chemistry and Application of Dyes, Springer, p. 381 (1990).
13. J. Kunitomo and M. Satoh, *Chem. Pharm. Bull.*, **30**, 2659 (1982); https://doi.org/10.1248/cpb.30.2659
14. X. Zhang, W. Ye, S. Zhao and C.-T. Che, *Phytochemistry*, **65**, 929 (2004); https://doi.org/10.1016/j.phytochem.2003.12.004
15. E. Corey and D.Y. Gin, *Tetrahedron Lett.*, **37**, 7163 (1996); https://doi.org/10.1016/0040-4039(96)01622-X
16. J.S. Yadav, B.V.S. Reddy, K.S. Raj and A.R. Prasad, *Tetrahedron*, **59**, 1805 (2003); https://doi.org/10.1016/S0040-4020(03)00076-0
17. Z. Zalán, T.A. Martinek, L. Lázár and F. Fülöp, *Tetrahedron*, **59**, 9117 (2003); https://doi.org/10.1016/j.tet.2003.09.062
18. J.D. Scott and R.M. Williams, *Chem. Rev.*, **102**, 1669 (2002); https://doi.org/10.1021/cr010212u
19. P. Craig, F. Nabenhauer, P. Williams, E. Macko and J. Toner, *J. Am. Chem. Soc.*, **74**, 1316 (1952); https://doi.org/10.1021/ja01125a051
20. M.C. Francisco, A.L.M. Nasser and L.M. Lopes, *Phytochemistry*, **62**, 1265 (2003); https://doi.org/10.1016/S0031-9422(02)00655-6
21. H. Kubota, T. Watanabe, A. Kakefuda, N. Masuda, K. Wada, N. Ishii, S. Sakamoto and S. Tsukamoto, *Bioorg. Med. Chem.*, **12**, 871 (2004); https://doi.org/10.1016/j.bmc.2003.12.032
22. A. Hegedüs and Z. Hell, *Tetrahedron Lett.*, **45**, 8553 (2004); https://doi.org/10.1016/j.tetlet.2004.09.097
23. Z.Y. Kadhim, A.N. Seewan, M.T. Abd and H.R. Saud, *Int. J. Pharm. Res.*, **12**, 402 (2020); https://doi.org/10.31838/ijpr/2020.12.03.062
24. L. Collins and S.G. Franzblau, *Antimicrob. Agents Chemother.*, **41**, 1004 (1997); https://doi.org/10.1128/AAC.41.5.1004

25. V.M. Kumbar, M.R. Peram, M.S. Kugaji, T. Shah, S.P. Patil, U.M. Muddapur and K.G. Bhat, *Odontology*, **109**, 18 (2021); https://doi.org/10.1007/s10266-020-00514-y

26. S. Sahana, G. Vijayakumar, R. Sivakumar, D. Sriram and D. Saiprasad, *J. Korean Chem. Soc.*, **66**, 194 (2022); https://doi.org/10.5012/jkcs.2022.66.3.194

27. A. Daina, O. Michielin and V. Zoete, *Sci. Rep.*, **7**, 42717 (2017); https://doi.org/10.1038/srep42717

28. A. Daina, O. Michielin and V. Zoete, *J. Chem. Inf. Model.*, **54**, 3284 (2014); https://doi.org/10.1021/ci500467k

29. A. Daina and V. Zoete, *ChemMedChem*, **11**, 1117 (2016); https://doi.org/10.1002/cmdc.201600182

30. D.A. Filimonov and V.V. Poroikov, Bioactive Compounds Design: Possibilities for Industrial Use, BIOS Scientific Publishers: Oxford U.K., p. 47 (1996).

31. R.K. Goel, D. Singh, A. Lagunin and V. Poroikov, *Med. Chem. Res.*, **20**, 1509 (2011); https://doi.org/10.1007/s00044-010-9398-y

32. N. Khurana, M.P.S. Ishar, A. Gajbhiye and R.K. Goel, *Eur. J. Pharmacol.*, **662**, 22 (2011); https://doi.org/10.1016/j.ejphar.2011.04.048

33. B.S. Furniss, A.J. Hannaferd, V. Rogers, P.W.G. Smith and A.R. Tatchell, Vogel's Textbook of Practical Organic Chemistry, Longman, Inc.: New York, Edn. 14 p. 716 (1981).

34. L.-T. Lin, W.-C. Hsu and C.-C. Lin, *J. Tradit. Complement. Med.*, **4**, 24 (2014); https://doi.org/10.4103/2225-4110.124335

35. G. Bickerton, G. Paolini, J. Besnard, S. Muresan and A. Hopkins, *Nat. Chem.*, **4**, 90 (2012); https://doi.org/10.1038/nchem.1243